Analysis of Concentration Fluctuations from Lidar Observations of Atmospheric Plumes

W. S. LEWELLEN AND R. I. SYKES

Aeronautical Research Associates of Princeton, Inc., Princeton, NJ 08540

(Manuscript received 14 September 1985, in final form 13 January 1986)

ABSTRACT

A series of nearly instantaneous vertical cross sections of power-plant plume concentrations obtained by both airborne and ground-based lidar systems for the Electric Power Research Institute (EPRI) Plume Model Validation and Development Project have been analyzed. By statistically resampling the data, values of the ratio of the ensemble rms concentration fluctuation, σ_c, to the ensemble mean concentration, $\bar{c}$, near the center of the plumes are found to vary from 0.2 to 4. More importantly, it is found that the normalized probability distribution function can be well represented as that resulting from a Gaussian distribution with any nonrealizable negative tail replaced by a delta function, representing intermittency at zero.

1. Introduction

Atmospheric plume dispersion is driven by the combination of transport by the wind and diffusion by the turbulence. However, a clear-cut division of the atmosphere's motions into a transporting wind and diffusing turbulence is not generally possible. Much of the atmosphere's motion in the transition range of sizes results in random motions of the plume, which may contribute to transport or diffusion depending upon the plume spatial scale and the sampling time scale. These transition motions also introduce an unpredictability into the dispersion of the plume. Lewellen and Sykes (1983) proposed a procedure for estimating this plume predictability. Our procedure is based on three steps: 1) the use of an assumed probability distribution function to interpret the time-averaged variance as a measure of expected uncertainty in sample observations; 2) the determination of the relationship between the ensemble variance and the variance in a particular time-averaged sample; and 3) the prediction of the ensemble variance. We have proposed models for accomplishing step 3 in Sykes et al. (1984, 1985) and a model for step 2 in Sykes (1984). Here we analyze available plume data to determine typical values of concentration fluctuations and to provide a data base for the choice of the probability distribution function necessary for step 1.

In recognition of the potential value of accurate model simulations of the dispersions of plumes from power plants, EPRI has undertaken a Plume Model Validation and Development Project (PMVD) (Hilst, 1978). A summary of the result from phase I of this project has been given by Bowne et al. (1983). Remote sensing by both airborne and ground-based lidars have been an integral part of the extensive field measurement program. These instruments, described in detail by Uthe (1983; airborne) and Hawley et al. (1983; ground-based), have the capability of recording a large number of near-instantaneous scans of a dispersing plume. The power plant stacks are large, approximately 200 m tall with exit diameters of approximately 10 m. This project provides a large block of data on concentration fluctuations in real atmospheric plumes under a number of different conditions. We have statistically analyzed the most available part of this data base and the results are presented here.

The number of individual scans in any one hour is approximately 10, so a straightforward calculation of the variance is unreliable. However, by using the hypothesis that the spatial shape of the near-instantaneous plume scan is uncorrelated with the centroid position of the individual scan, we can use statistical resampling to expand the effective sample size and obtain consistent estimates of the rms concentration fluctuation σ_c as well as the mean $\bar{c}$. Our resampling is justified as long as the small-scale eddies which control the detailed shape of an individual scan are uncorrelated with the larger-scale wind fluctuations that dominate the centroid movement. Examples of the raw individual scans and the resulting spatial distributions of σ_c and $\bar{c}$ for given times are shown in section 2. At any given time the minimum value of $\sigma_c/\bar{c}$ (from 0.2 to 4) occurs near the center of the plume, with increasing values in the edges of the plume. The low values represent well-defined plumes under nocturnal conditions, while the large values occur under convective conditions. We interpret our results as only giving lower bound estimates for the larger values, since even our expanded sample size is inadequate to precisely determine large values of $\sigma_c/\bar{c}$.

We speculate that the probability distribution function of concentration fluctuation can be reasonably represented as a function of $\bar{c}$ and σ_c only. By using

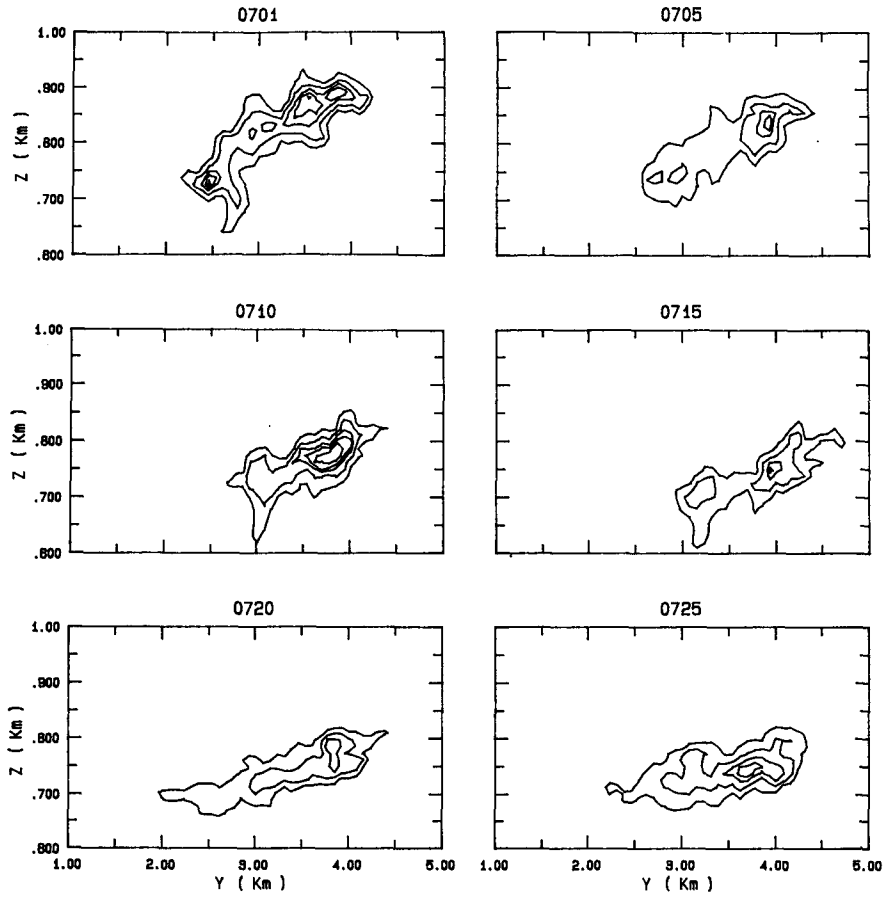

FIG. 1. Twelve individual, consecutive scans of the Kincaid power plant plume 10 km downwind of the stack between 0700 and 0800 GMT 4 May 1980 as observed by the Alpha 1 lidar. The same arbitrary normalization is used for all of the contours so that the relative contour levels are 2, 6, 10, 12, and 14.

our deduced values of σ_c and $\bar{c}$ to subdivide the real data into several bins with relatively narrow ranges of their value of $\sigma_c/\bar{c}$, we find a unique family of cumulative distribution functions. Further, we find that this cumulative distribution family may be closely parameterized as that resulting from a normal, Gaussian distribution with any nonrealizable negative concentration tail replaced by a delta function at zero concentration. This delta function represents the intermittency of the local concentration. Some theoretical justification for the clipped normal is given in the Appendix.

2. Analysis procedures

Typical cross sections of the individual scans for 1 h are given in Fig. 1. This series is taken by the Alpha 1 aircraft approximately 10 km downwind of the Kincaid power plant exhaust stack during early morning conditions.

The Alpha I instrument (Uthe, 1983) detects the back scatter from plume aerosols. The basic instrument limit on resolution is approximately 3 m in the vertical and 20 m in the horizontal. However, the background scatter from ambient atmospheric aerosols must be subtracted from the signal to obtain the signature of the plume. In some cases, we found the background signal to be so noisy that it was necessary to filter the data before a consistent background could be identified. In the worst cases, this filtering reduced the effective resolution of the data to 25 m in the vertical and 120 m in the horizontal. In Fig. 1, the effective resolution is 12 m in the vertical and 60 m in the horizontal.

A straightforward average of the scans in Fig. 1 is given in Fig. 2. This provides an estimate of the mean concentration distribution for the hour. However, the sample size is too small for any reliable estimate of the variance by a straightforward calculation. We use statistical resampling to expand the effective sample size.

In general there is considerable difference between the size of the relatively large-scale eddies that dominate the movement of the plume centroid and small-scale eddies that control the detailed shape of the concen-

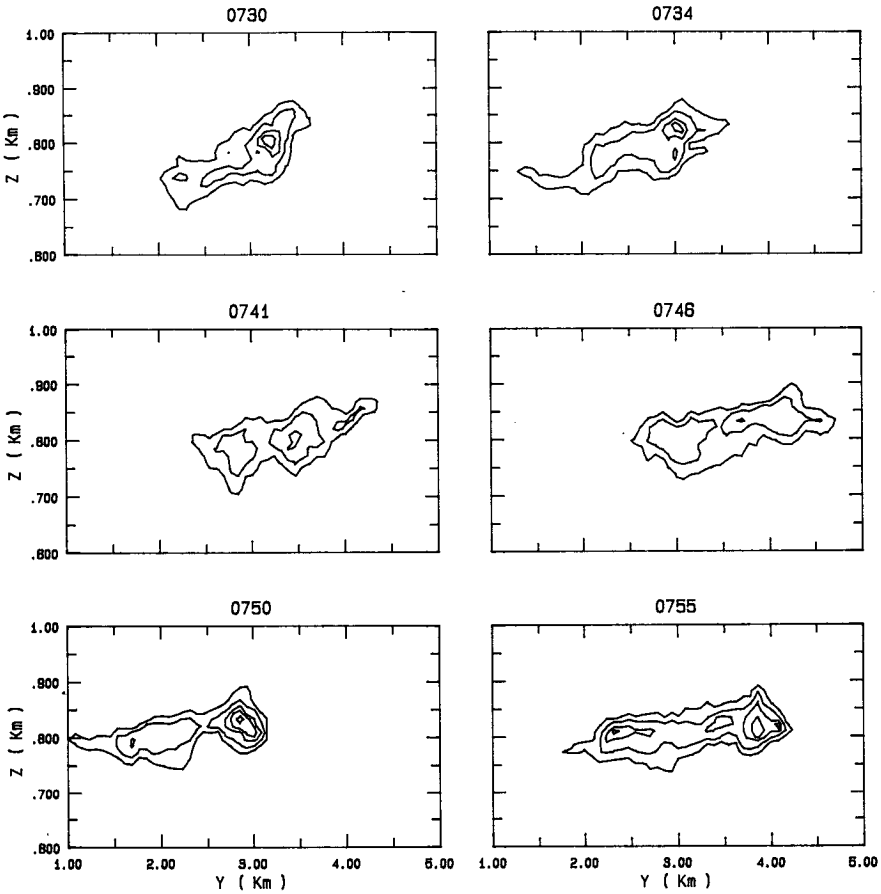

FIG. 1. (*Continued*)

tration distribution in any individual scan. This spread in eddy sizes should lead to the detailed shape of the individual scans being very poorly correlated with the centroid movement. By using the hypothesis that the shape of the near-instantaneous plume scan is completely uncorrelated with the centroid position of the individual scan, we can effectively square the sample size for resampling. Thus each scan centroid position relative to a fixed point in space is combined with each scan distribution about its centroid to increase our sample size from N to N^2. Note that our mean concentration and variance includes the meander component as well as the instantaneous shape fluctuations.

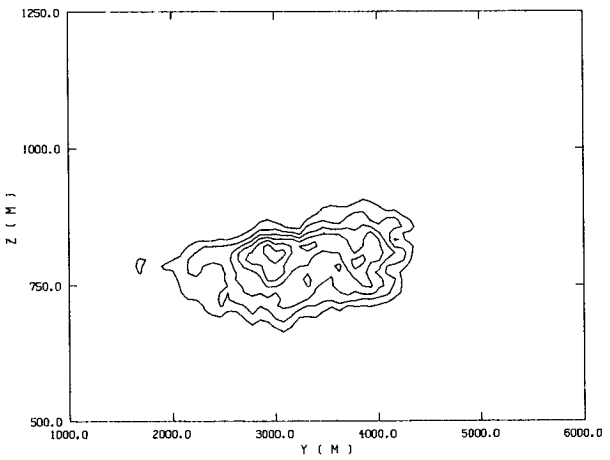

FIG. 2. Average of the individual scans shown in Fig. 1 with six contours at relative levels of 0.8, 1.6, 2.4, 3.2, 4, and 4.8.

The average of 144 samples created from the scans given in Fig. 1 is presented in Fig. 3. This figure is smoother than Fig. 2 and has lower maximum values; we regard Fig. 3 as a truer estimate of the ensemble mean distribution for the hour than that given by Fig. 2. That is, if the experiment could be repeated many times with the nominal meteorological and emissions conditions held fixed, then Fig. 3 is a better estimate of the mean distribution. More significantly, the sample size is now sufficiently large that we can obtain a reasonably smooth distribution of the standard deviation from this mean in the 144 samples as given in Fig. 4. The absolute value of any of the contours in these first

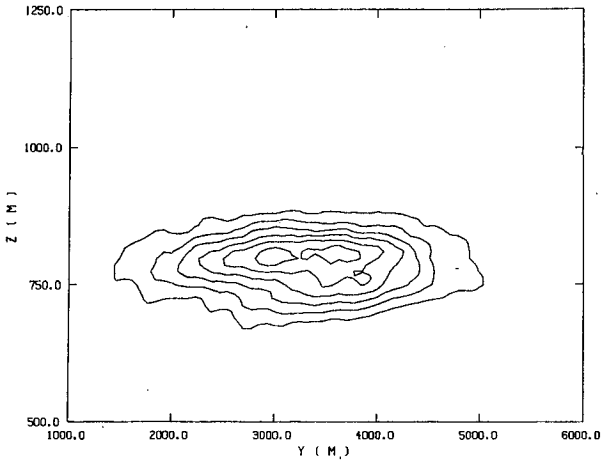

FIG. 3. Average of the resampled data for the hour shown in Fig. 1 using the procedure detailed in section 2 with six contours at relative levels of 0.5, 1, 1.5, 2, 2.5, and 3.

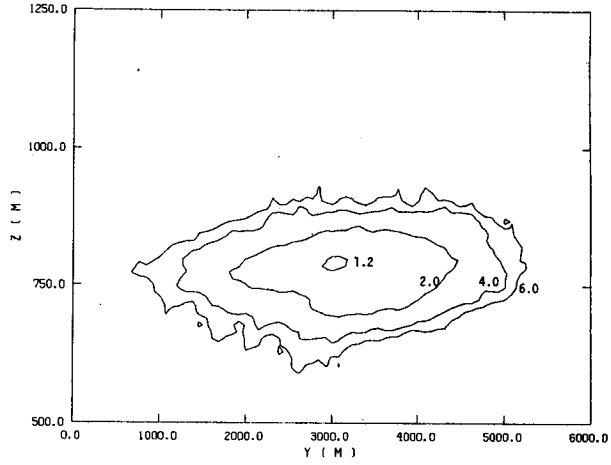

FIG. 5. The ratio of σ_c shown in Fig. 4 to the $\bar{c}$ shown in Fig. 3.

four figures is of little interest since the Alpha 1 lidar is recording the relative concentration of aerosol within the plume. What is of interest is the ratio of the standard deviation of the concentration, σ_c, to its mean value $\bar{c}$. This distribution is shown in Fig. 5. Figure 5 shows a minimum for $\sigma_c/\bar{c}$ near the center of the plume with generally increasing values with increasing distance from the plume center.

The above procedure has been performed on 24 h of Alpha 1 data and 86 h of Dial data. The Dial data are taken from both the Kincaid and Bull Run data sets. The Dial instrument measures the plume SO_2 contribution and is archived in the PMVD data base. It has a resolution of approximately 15 m in the vertical and horizontal. Before describing the $\sigma_c/\bar{c}$ results, we will describe the procedure used to obtain probability distribution functions from this data.

The critical choice which must be made in generating any probability distribution function, pdf, is how the data are to be combined. Since $\sigma_c/\bar{c}$ shows such a strong spatial dependence, we feel it is important not to combine all the samples for an hour into one distribution function. Rather, we wish to test the hypothesis that the ensemble pdf can be reasonably represented as a normalized function of $\sigma_c/\bar{c}$ only. Our deduced values of σ_c and $\bar{c}$ in Figs. 3 and 4 are used to subdivide the real data in Fig. 1 into bins with relatively narrow ranges of their value of $\sigma_c/\bar{c}$. For example, the data of Fig. 1 can be segregated by combining the data which fall within an annular region designated by a narrow range of values of $\sigma_c/\bar{c}$. Note that although the resampled data are used in generating σ_c and $\bar{c}$, only the original sample points are used in generating the cumulative distribution function of Fig. 6. Of course, the resampling procedure can still affect the distribution through its influence on σ_c and $\bar{c}$. Data points from the

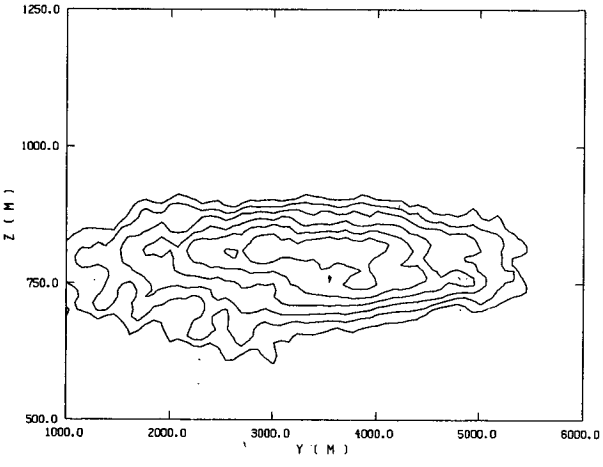

FIG. 4. The standard deviation of the resampled data from the mean shown in Fig. 3 with six contours at relative levels of 0.6, 1.2, 1.8, 2.4, 3, and 3.6.

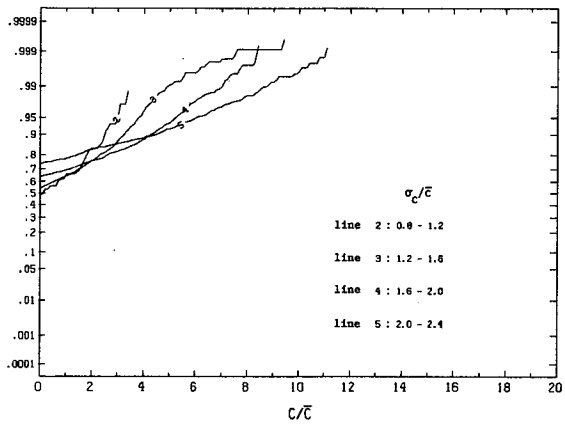

FIG. 6. Cumulative distribution functions for the data of Fig. 1 segregated by intervals of $\sigma_c/\bar{c}$.

TABLE 1. Near centerline values of $\sigma_c/\bar{c}$.*

Date/Hour	d(km) from stack	sg(c)/cb	q (m s^{-1})	w_s (m s^{-1})
	Dial Kincaid			
15 May 1981				
0400	2.0	0.96	na	9.62
0500	3.0	0.63	na	9.00
0700	3.0	0.91	na	7.33
16 May 1981				
0200	1.5	0.22	na	8.88
0300	0.9	0.22	na	8.94
0400	1.4	0.54	na	8.72
0500	1.4	0.98	na	8.37
0600	1.5	0.97	na	7.83
0700	1.2	0.96	na	6.74
0800	0.9	0.75	na	6.03
0900	1.1	0.70	na	5.74
1000	0.8	0.94	na	6.27
24 May 1981				
2000	1.2	0.45	1.89	6.64
2100	1.1	0.85	1.92	5.77
2200	1.1	1.07	1.5	5.42
28 May 1981				
1700	1.8	1.87	1.87	3.87
1900	1.1	0.91	1.55	5.54
31 May 1981				
0200	2.9	0.48	1.39	4.09
0300	3.2	1.03	2.26	3.48
0400	2.5	1.32	1.85	3.28
0600	2.3	0.57	1.37	4.20
0700	2.9	0.61	1.49	4.48
0800	3.0	0.80	1.57	4.85
1 Jun 1981				
0200	3.2	0.59	1.96	8.40
0400	3.3	0.59	1.65	8.19
0500	3.3	0.45	1.83	8.30
	Dial Bull Run			
15 Oct 1982				
1200	1.56	0.83	na	4.76
1300		1.33	na	4.90
1400		1.22	1.84	5.10
1500		1.08	1.91	5.60
1600		1.78	2.08	6.29
1700		0.92	2.17	6.78
1800		0.79	1.76	7.21
1900		0.95	1.00	7.36
16 Oct 1982				
1000	0.92	1.20	1.00	3.75
1100		1.21	1.48	3.88
1200		1.15	1.58	4.16
1300		1.46	1.70	4.22
1400		1.43	1.88	5.13
1500		1.04	1.79	6.43
1600		0.70	1.69	7.32
1700		0.95	1.54	7.35
1800		0.88	1.36	7.00
18 Oct 1982				
0400	1.56	0.48	0.30	0.97
0500		0.45	0.35	0.92
0600		0.42	0.32	1.40
0700		0.41	0.30	1.64
0800		0.51	0.35	1.91
0900		0.47	0.32	1.78
1000		0.54	0.44	1.62
1100		0.52	0.62	1.88
1200		0.65	0.89	2.22

Date/Hour	d(km) from stack	sg(c)/cb	q (m s^{-1})	w_s (m s^{-1})
	Alpha 1 Kincaid			
4 May 1980				
0600	10	0.76	0.82	4.42
0700	10	1.28	0.87	4.72
0800	10	0.89	1.04	3.75
0900	10	1.97	1.01	2.96
1000	10	>2.60	1.39	2.76
5 May 1980				
0600	16	1.86	1.52	9.34
0700	16	1.04	2.52	7.30
0800	20	0.74	1.89	4.76
0900	17	1.37	1.85	5.05
1000	17	>3.33	2.12	6.36
9 May 1980				
1300	7	>3.78	2.01	3.75
1400	7	>2.46	3.33	4.37
20 Jul 1980				
0800	11	1.02	1.51	7.98
0900	11	1.42	1.39	7.98
24 Jul 1980				
0800	9	0.46	1.42	4.03
0900	9	1.16	2.53	2.89
1000	9	>1.36	1.45	2.75
16 May 1981				
0400	12	0.63	na	8.72
0500	13	1.05	na	8.37
24 May 1981				
2000	14–15	1.63	1.89	6.64
2100	14–15	2.08	1.92	5.77
28 May 1981				
1900	3	1.58	1.55	5.54
5 Oct 1982				
1100	1.56	0.60	0.49	1.54
1200		1.01	0.68	1.59
1300		1.38	0.95	1.83
1400		1.50	0.96	1.78
1500		1.39	0.71	1.41
1600		1.30	0.58	1.26
1700		1.19	0.52	1.02
1800		0.92	0.32	0.91
1900		1.07	0.14	0.84
6 Oct 1982				
1500	1.56	1.08	0.99	1.33
1600		1.45	0.71	1.67
1700		1.23	0.65	2.07
1800		0.80	0.46	2.42
1900		0.50	0.26	2.76
2000		0.50	0.30	3.34
2100		0.40	0.33	4.10
2200		0.93	0.35	4.89
2300		0.37	0.39	5.62
9 Oct 1982				
1500	1.56	0.82	1.37	5.61
1600		2.05	1.34	5.46
1700		1.54	1.14	4.74
1800		0.70	0.86	3.72
1900		0.63	0.45	3.62
10 Oct 1982				
1000	1.56	0.54	0.55	3.03
1100		0.64	0.88	3.09
1200		2.09	0.95	3.15
1300		0.73	0.88	3.05
1400		0.87	0.80	2.64
1600		1.63	0.71	2.69
1700		0.78	0.73	3.02
1800		0.85	0.69	3.38

* sg(c)/cb computed as the average of σ_c over the average of $\bar{c}$ for the set of data points with $\bar{c} > 0.8\bar{c}_{max}$.

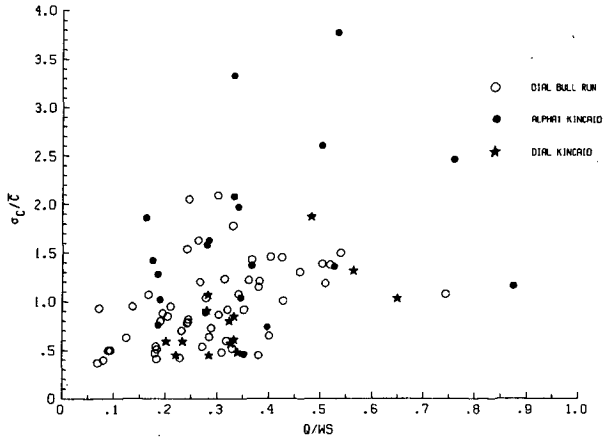

FIG. 7. Plot of the intensity of the concentration fluctuations versus the intensity of the wind fluctuations. Note that the values are taken at different distances from the stack as indicated in Table 1.

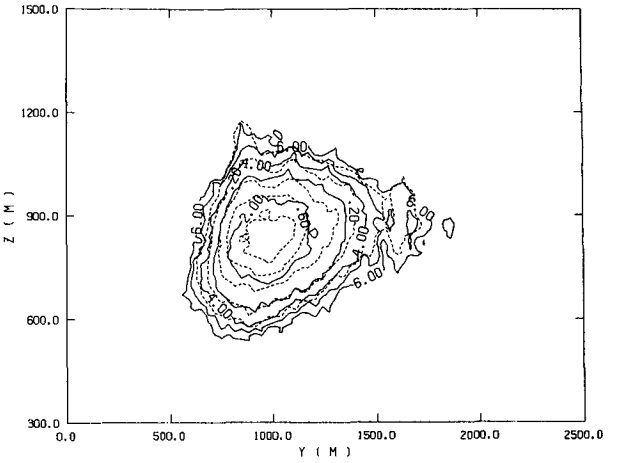

FIG. 9. Normalized concentration as observed by Alpha 1 between 1900 and 2000 GMT on 28 May 1981 with contours of $\sigma_c/\bar{c}$ superimposed. Dashed contours of $\bar{c}/\bar{c}_{max}$ for 0.1, 0.2, 0.4, 0.6, 0.8; solid contours of $\sigma_c/\bar{c}$ for 1.0, 2.0, 3.0, 4.0, 5.0, 6.0.

region of larger $\sigma_c/\bar{c}$ values show consistently larger values of intermittency and flatter distribution curves. Thus the pdf, at least, is a strong function of $\sigma_c/\bar{c}$. It remains to be seen how unique a function it is.

This completes the specification of the general procedure used to obtain the results of section 3. We analyzed all of the Dial vertical scan data that were available from the PMVD data base both from the Kincaid, plains site and from the Bull Run, moderately complex site. The Alpha 1 data were treated more selectively. All of the data were reviewed in the picture book format described by Uthe (1983), and 24 h were chosen on the basis of large signal-to-background noise ratio and a sufficient number of scans taken at the same plume position to warrant this statistical approach.

In experimenting with the data analysis we attempted to adjust for any movement of the plumes centroid by a mean wind shift during the hour being analyzed. The mean wind was approximated by filtering the tower observations using a triangular running average over $\pm 1\frac{1}{2}$ hours. There were no significant differences between the results with this mean wind adjustment and those without it.

The most serious problem with the Dial data appeared to be some self-shielding of the plume under conditions of large concentrations. This appears in some of the scans as a premature cutoff of the concentration contours on the back side of the plume. The hours when this problem was most apparent in the individual scans have been eliminated from the results presented in section 3.

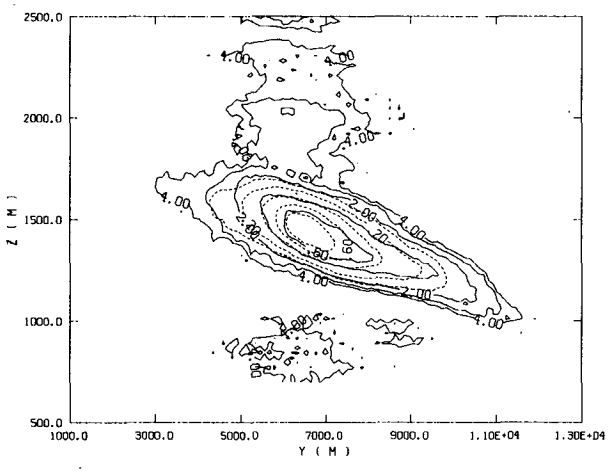

FIG. 8. Normalized concentration as observed by Alpha 1 between 0800 and 0900 GMT 24 July 1980 with contours of $\sigma_c/\bar{c}$ superimposed. Dashed contours of $\bar{c}/\bar{c}_{max}$ for 0.1, 0.2, 0.4, 0.6, 0.8; solid contours of $\sigma_c/\bar{c}$ for 0.6, 1.0, 2.0, 4.0.

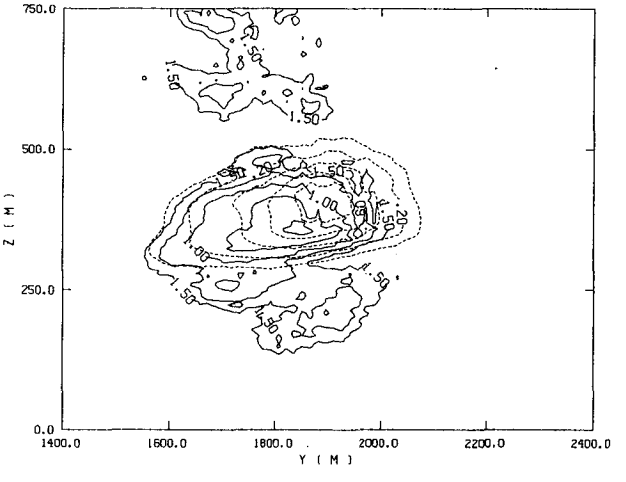

FIG. 10. Normalized concentration as observed by Dial between 0700 and 0800 GMT 16 May 1981 at Kincaid with contours of $\sigma_c/\bar{c}$ superimposed. Dashed contours of $\bar{c}/\bar{c}_{max}$ for 0.1, 0.2, 0.4, 0.6, 0.8; solid contours of $\sigma_c/\bar{c}$ for 0.5, 0.75, 1, 1.25, 1.5.

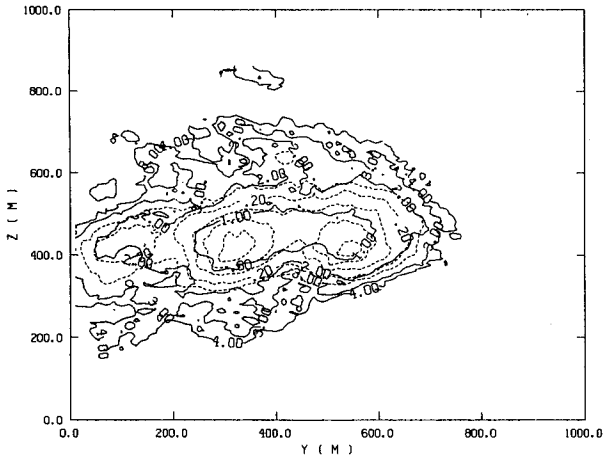

FIG. 11. Normalized concentration as observed by Dial between 1800 and 1900 GMT on 9 October 1982 at Bull Run with contours of $\sigma_c/\bar{c}$ superimposed. Dashed contours of $\bar{c}/\bar{c}_{max}$ for 0.1, 0.2, 0.4, 0.6, 0.8; solid contours of $\sigma_c/\bar{c}$ for 1.0, 2.0, 3.0, 4.0.

3. Results

a. *Fluctuation distribution*

A summary of the values of $\sigma_c/\bar{c}$ near the plume center are given in Table 1. These results are grouped by instrument and site. The hour observed and the distance from the source point are also included. The actual value of $\sigma_c/\bar{c}$ tabulated is the ratio of the average of the values occurring within the $\bar{c}/\bar{c}_{max} = 0.8$ contour. The lowest value of $\sigma_c/\bar{c}$ analyzed is 0.2 and the highest, 4. The smallest value was obtained from the Dial observations during nocturnal conditions with a relatively strong, steady wind. The high value was obtained by the Alpha 1 under afternoon conditions. The low value is probably a reasonable estimate of minimum expected values of $\sigma_c/\bar{c}$, but the high value is probably a poor estimate of the upper bound on $\sigma_c/\bar{c}$. The data are biased against higher values for two reasons. The instrumental limitation of approximately 10 scans per hour means that higher values of $\sigma_c/\bar{c}$ will be very poorly defined. Due to this poorer quality of data under conditions where the higher values of $\sigma_c/\bar{c}$ may be expected, the field experiment was set to generally utilize vertical scans with these instruments under favorable signal-to-noise conditions. Consequently, the largest values of plume centerline $\sigma_c/\bar{c}$ that occurred during the EPRI PMV&D intensive field tests are undoubtedly not included in Table 1. The symbol $\geq$ in Table 1 indicates that the estimate is approximate because the distributions are quite ragged and the real value is likely to be higher than this.

The wind speed w_s, and turbulent velocity, q, as taken from the 100 m level of a meteorological tower near each stack, are also given in Table 1. There is some correlation between the turbulent intensity as measured by q/w_s parameters and the value of $\sigma_c/\bar{c}$, but there is a lot of scatter as seen in Fig. 7. We do not believe the few parameters provided in Table 1 provide enough information to explain the observed variation in $\sigma_c/\bar{c}$. Rather, this information is provided to demonstrate that the data were taken over varied conditions. In spite of this, it will be shown subsequently that the pdf from all of this data can be represented by the same function.

Some sample distributions of normalized concentration are shown in Figs. 8 to 11 with contours of $\sigma_c/\bar{c}$ superimposed. Figure 8 shows an hour with smooth inner contours and low minimum values of $\sigma_c/\bar{c}$. Figure 9 shows an hour with significantly larger values of $\sigma_c/\bar{c}$. Figure 10 shows an hour of the Dial Kincaid data where there is some problem with self-shielding and Fig. 11 shows a case where the Bull Run Dial data exhibits a bifurcation of the mean plume.

The clue that there is some problem with Fig. 10 is that there is an offset between $\bar{c}$ and the $\sigma_c/\bar{c}$ curves. This is even more apparent in the original σ_c and $\bar{c}$ plots. The values of $\bar{c}$ drop off much faster to the right of the maximum than they do to the left. When the individual scans are shifted in the resampling process this forces the values of σ_c to be increased on the right side and results in the observed shift in the minimum of $\sigma_c/\bar{c}$ away from the region of maximum $\bar{c}$. Figure 10 represents a marginal data hour that was included in the sample. Hours where the self-shielding was obviously worse than that in Fig. 10 were removed from the data set.

b. *Probability distribution functions*

We test the hypothesis that the pdf can be reasonably represented when the σ_c and $\bar{c}$ are given. When normalized by $\bar{c}$ the cumulative distribution functions appear to become a function of $\sigma_c/\bar{c}$ only. This is demonstrated in Fig. 12 where the cdf's for the different hours shown in Figs. 8–11 are plotted on the same figure after the data have been sorted according to their analyzed value of $\sigma_c/\bar{c}$. Each group represents an interval of 0.4 in $\sigma_c/\bar{c}$. The most notable differences between the individual hour distributions involve the curves labeled 3 which are shown for the hour in Fig. 10. As previously discussed, the results for this case are suspect, due to some probable self-shielding of the Dial data. It is remarkable that data taken from the center of the plume in Fig. 9 shows nearly the same pdf as data taken from the edges of the plume in Fig. 8. Based on this similarity all the data are combined in Fig. 13. Three curves are given for each $\sigma_c/\bar{c}$ interval—one for the Alpha 1 data, one for the Kincaid Dial data, and one for the Bull Run Dial data. Again, each group represents an interval of $\sigma_c/c = 0.4$. The only real differences in these distributions are for extreme values at probabilities above 0.99.

We have also included ideal clipped normal distributions in Figs. 12 and 13 for the values of $\sigma_c/\bar{c}$ marking the boundaries between the respective intervals. These

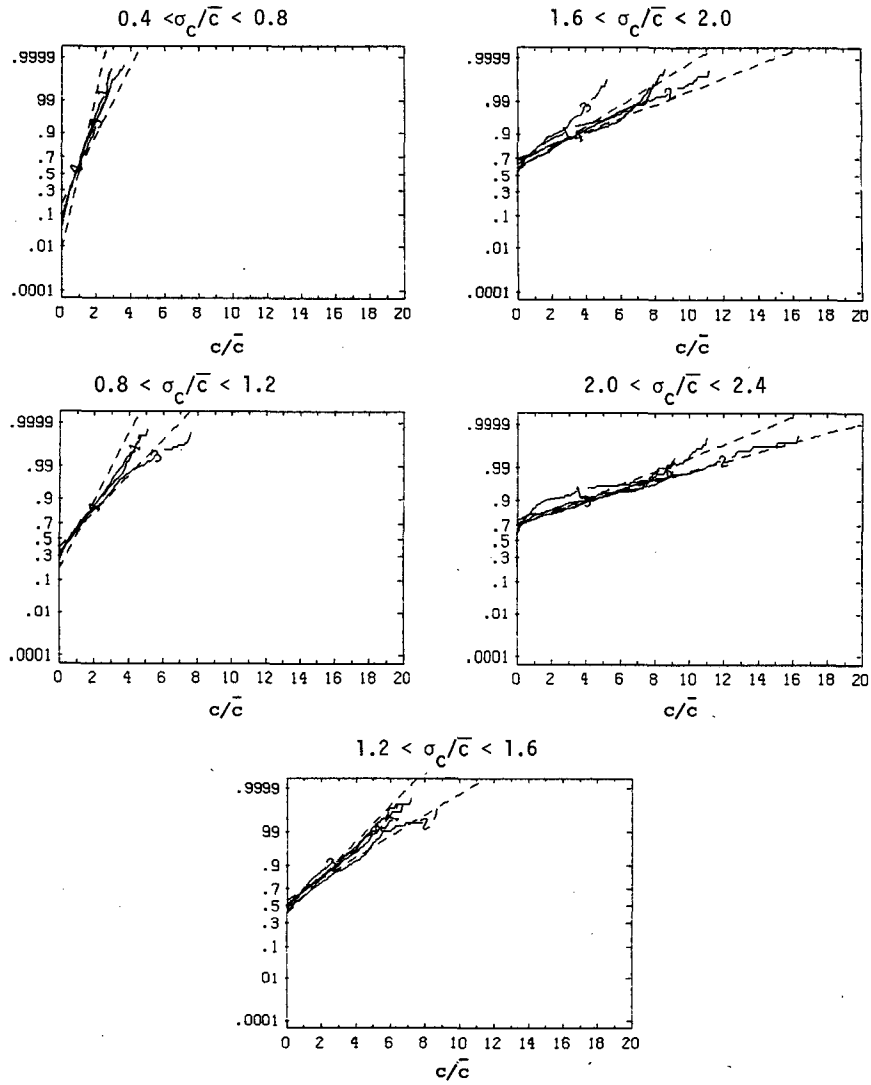

FIG. 12. Cumulative distribution functions for the data taken during the hours exhibited in Figs. 8–11 segregated according to $\sigma_c/\bar{c}$ interval. Dashed lines are for the ideal clipped normal boundaries.

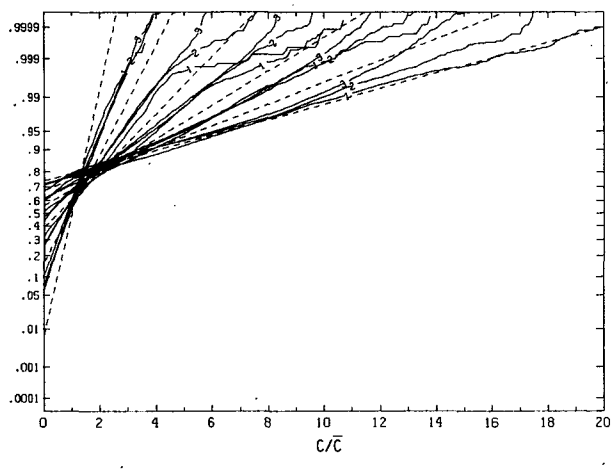

FIG. 13. Cumulative distribution functions for all data. (1: Alpha 1 data, 2: Dial Kincaid, 3: Dial Bull Run). The dashed lines are ideal bin boundaries as derived from a clipped normal distribution with $\sigma_c/\bar{c} = 0.4$ to 2.4 at intervals of 0.4.

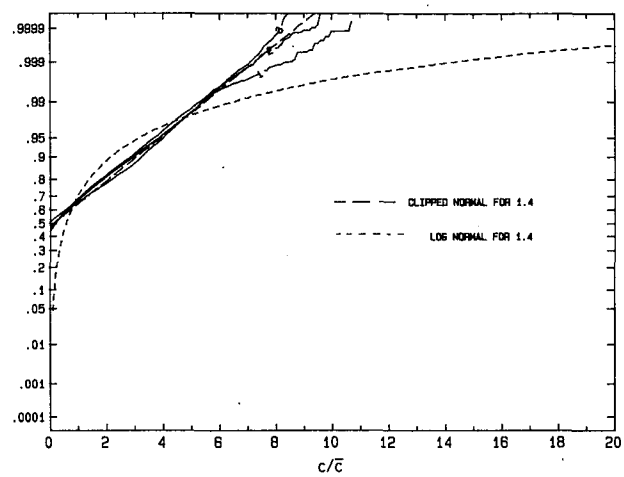

FIG. 14. Comparison between the lognormal cdf and the clipped normal cdf for $\sigma_c/\bar{c} = 1.4$. The observed cdf's for the three different sites for the range $1.2 < \sigma_c/\bar{c} < 1.6$ are also included.

theoretical curves are seen to fall neatly between the appropriate corresponding observed cdf's. With the exception of a couple of the tails, the curves do not stray outside the range designated for their particular $\sigma_c/\bar{c}$ interval.

The observed cdf are noticeably closer to the ideal clipped normal distribution than that of a lognormal distribution, as demonstrated in Fig. 14. The data for $\sigma_c/\bar{c} > 1$ could be reasonably well fit by the combination of an exponential distribution and an intermittency parameter, but values of $\sigma_c/\bar{c} < 1$ would have to be excluded. The clipped normal provides a good representation of the data and a smooth transition for the full range of possible values of $\sigma_c/\bar{c}$. We believe Figs. 13 and 14 provide strong justification for using the clipped normal distribution to parameterize the general dependence of concentration pdf on $\sigma_c/\bar{c}$ as used by Lewellen et al. (1984). A theoretical foundation for the clipped normal distribution is presented in the Appendix.

4. Conclusions

Analysis of a relatively large block of lidar data shows that at any given time the minimum value of the ratio of the ensemble rms concentration fluctuation σ_c to the ensemble mean concentration $\bar{c}$ is likely to be of order 1. Analyzed values near the plume center varied from 0.2 to 4.

We find that the normalized probability distribution functions can be closely parameterized as a unique function of $\sigma_c/\bar{c}$ and that this function is remarkably close to that resulting from a normal Gaussian distribution with any nonrealizable negative tail replaced by a delta function, representing intermittency at zero.

Acknowledgments. This research was supported by EPRI as part of its Plume Model Validation and Development Project under the direction of Glenn Hilst. Detailed data analysis was provided by Hilda Philander and help was provided by Harvey Segur in the Appendix.

Theoretical Support for the Clipped Normal Distribution

A rational way of estimating a pdf for any given data set is to choose the pdf with the minimum information (maximum entropy) that satisfies the known constraints (Tribus, 1969). We choose to impose five constraints:

(i) No negative concentrations

$$p = 0, \quad x < 0; \tag{A1}$$

(ii) a finite probability of zero concentration denoted by A, so that

$$\int_0^\infty p d\chi = 1 - A; \tag{A2}$$

(iii) a specified mean, μ,

$$\int_0^\infty \chi p d\chi = \mu; \tag{A3}$$

(iv) a specified variance, σ^2,

$$\int_0^\infty \chi^2 p d\chi = \sigma^2 + \mu^2; \tag{A4}$$

(v) and intermittency uniquely determined as a function of σ/μ,

$$A = A(\sigma/\mu). \tag{A5}$$

The first four of these constraints are straightforward; the fifth is added because we wish to introduce intermittency without adding any additional independent parameters.

When the entropy,

$$S = -\int_0^\infty p \ln p d\chi \tag{A6}$$

is maximized subject to (i)–(v) it is necessary to have

$$p = \exp - [(\lambda_0 + \lambda_1\chi + \lambda_2\chi^2)] \tag{A7}$$

where λ (Lagrange multipliers) are determined by the constraints. We can arbitrarily replace the three constants λ_0, λ_1, and λ_2 in Eq. (A7) with three new constants, κ, μ_0, and σ_0 so that

$$p = \frac{1}{\kappa\sigma_0} \exp - (x - \mu_0)^2/2\sigma_0^2. \tag{A8}$$

The constraints imposed by Eqs. (2) through (4) may now be written as

$$A = 1 - \frac{\sqrt{2\pi}}{2\kappa}[1 + \mathrm{erf}(\mu_0/\sigma_0\sqrt{2})], \tag{A9}$$

$$\mu = \frac{\sigma_0}{\kappa} \exp [-(\mu_0^2/2\sigma_0^2)] + \mu_0(1 - A), \tag{A10}$$

$$\sigma^2 = -\mu^2 + \sigma_0^2(1 - A) + \mu_0\mu. \tag{A11}$$

When μ and σ are specified, Eqs. (9) through (11) are adequate to determine σ_0, μ_0, and A as functions of κ. However, from Eq. (5), we require the stronger constraint, namely that it be adequate to specify A uniquely. This can be most readily achieved by requiring that κ be a universal constant. If κ is set equal to $\sqrt{2\pi}$, then all the constraints are satisfied and Eqs. (9) and (10) are the identical equations that relate the mean, μ, and standard deviation, σ, of a clipped normal distribution, defined as

$$p = \frac{1}{\sigma_0\sqrt{2\pi}} e^{-(x-\mu_0)^2/2\sigma_0^2}, \qquad \chi > 0$$

$$A = \frac{1}{2}[1 - \mathrm{erf}(\mu_0/\sigma_0\sqrt{2})], \quad \chi = 0$$

$$p = 0, \qquad \chi < 0 \tag{A12}$$

to the mean, μ_0, and standard deviation, σ_0, of the total unclipped normal distribution.

If we had chosen κ to be a function of σ/μ, the form of Eq. (13) would be altered. Although this yields an $A(\sigma/\mu)$ that is quite reasonable, we must appeal to the data comparison of Fig. 12 for real justification of this assumption.

We could reformulate the problem without the fifth constraint. It can be shown that leaving A completely free requires adding a term of $-A \ln A$ to S in Eq. (6). Now when A is varied to maximize S one finds that

$$A = e^{-\lambda_0}.$$

This results in a distribution which is almost identical to that of Eq. (13) when $\sigma/\mu \leqslant 1$, but departs significantly when $\sigma/\mu \gg 1$. The data of Fig. 13 has a clear preference for the A of Eq. (10) rather than eliminating Eq. (5) from the list of constraints.

REFERENCES

Bowne, N. E., R. J. Londergan, D. R. Murray and H. S. Borenstein, 1983: Overview, results, and conclusions for the EPRI Plume Model Validation and Development Project: Plains site. EPRI EA-3074, Research Project 1616-1, Final Rep., Electric Power Research Institute, Palo Alto, CA 227 pp.

Hawley, J. G., G. F. Wallace, L. D. Fletcher, C. J. Prior and J. B. Sheldon, 1983: Differential absorption lidar measurements of SO_2 at the Flat-Terrain Site—PMV&D Project. EPRI EA-3072 Research Project RP1616-12, Electric Power Research Institute, Palo Alto, CA, 144 pp.

Hilst, G. R., 1978: Plume model validation. EPRI Rep. EA-917-SY, Electric Power Research Institute, Palo Alto, CA.

Lewellen, W. S., and R. I. Sykes, 1983: On the use of concentration variance predictions as a measure of natural uncertainty in observed concentration samples. *Proc. Sixth Symp. on Turbulence and Diffusion,* Boston, Amer. Meteor. Soc., 47–50.

——, —— and S. F. Parker, 1984: An evaluation technique which uses the prediction of both concentration mean and variance. DOE/AMS Model Evaluation Workshop.

Sykes, R. I., 1984: The variance in time-averaged samples from an intermittent plume. *Atmos. Environ.,* **18,** 121–123.

——, W. S. Lewellen and S. F. Parker, 1983: A turbulent-transport model for concentration fluctuations and fluxes. *J. Fluid Mech.,* **139,** 193–218.

——, —— and ——, 1986: A Gaussian model of atmospheric dispersion based on second-order closure. *J. Climate Appl. Meteor.,* **25,** 322–331.

Tribus, M., 1969: *Rational Descriptions, Decisions and Designs.* Pergamon Press.

Uthe, E. E., 1983: Application of ALPHA-1 Plume Model Validation and Development—Plains Site. EPRI EA-3073 Research Project 1616-11, Final Rep., Electric Power Research Institute, Palo Alto, CA, 56 pp.